

COVER PAGE

Document downloaded by @DAEL

Sat Nov 28 09:22:11 2026
For personal use

When automatic English translation is provided, only the original document is authentic.
The EAA cannot be held responsible of any translation error

Bibliographical reference

Lamb Wave Propagation in a Piezoelectric/Piezomagnetic Bi-Material Plate with an Imperfect Interface, Guoquan Nie, Jinxi Liu and Xianglin Liu, Acta Acustica **vol. 102** (Number 5), 2016, pp. 893-901

DOI
https://doi.org/10.3813/AAA.919003

ACTA ACUSTICA UNITED WITH ACUSTICA
Vol. 102 (2016) 893 – 901
DOI 10.3813/AAA.919003

Lamb Wave Propagation in a Piezoelectric/Piezomagnetic Bi-Material Plate with an Imperfect Interface

Guoquan Nie[1)], Jinxi Liu[1)], Xianglin Liu[2)]
[1)] Department of Engineering Mechanics, Shijiazhuang Tiedao University, Shijiazhuang 050043, China.
niegq@stdu.edu.cn
[2)] Department of Mathematics and Physics, Shijiazhuang Tiedao University, Shijiazhuang 050043, China

Summary
Propagation of plane wave in a bi-material plate consisting of a piezoelectric layer and a piezomagnetic layer is investigated in this paper. The interface between the piezoelectric layer and the piezomagnetic layer is imperfectly bonded. By using the partial wave method, solutions to the governing equations of piezoelectric and piezomagnetic materials are obtained. The shear-lag model is used for describing the characteristics of bonding interface. Exact dispersion relations for four kinds of electro-magnetic boundary conditions are derived in matrix form. The influences of the electro-magnetic boundary condition, the interfacial parameter and the thickness ratio of piezoelectric layer to piezomagnetic layer on dispersion relations are also discussed. The numerical results show that the imperfect bonding of the interface can greatly affect the dispersion curve and generally reduce the wave velocity. The dispersion relations are more sensitive to the normal interfacial parameter comparing to the tangential parameter. The thickness ratio has great effect on the dispersion behavior. The obtained results are useful for the understanding and design of piezoelectric/piezomagnetic composites or structures for acoustic wave and microwave devices.

PACS no. 43.35.Pt

1. Introduction

Since the first artificial magneto-electro-elastic composite was grown by Suchtelen [1] in 1970s, some mechanics problems of such composites and structures have attracted great attention in recent years, which is due to the extensive applications for in microwave devices [2, 3, 4], sensors [5, 6, 7], transducers [8, 9], heterogeneous read/write devices [10], and so on. The related research advance was summarized by Fiebig [11] and Nan *et al.* [12] in their review papers. The layered composite made by piezoelectric material and piezomagnetic material is widely used in energy conversion and acoustic wave devices due to its relatively convenient preparation process. For the problem of elastic wave propagation in such structures, perfect bonding between piezoelectric and piezomagnetic materials is routinely assumed. Alshits *et al.* [13] first discussed the existence of surface wave in anisotropic piezoelectric/piezomagnetic half-space, and ten types of different boundary conditions that possibly exist in practical application were considered. Melkumyan [14] discovered that twelve different velocities of SH surface wave can be guided by the interface of two identical magneto-electro-elastic half-spaces with different mechanical and magneto-electrical boundary conditions. Liu *et al.* [15] and Wang *et al.* [16] almost at the same time found that SH surface wave can propagate in semi-infinite magneto-electric material adjoining a vacuum and the phase velocity of SH wave was also given in an explicit form. Soh and Liu [17] studied SH-type interface wave propagating in two perfectly bonded piezoelectric/piezomagnetic bi-material structure. Gusev *et al.* [18] studied the flexural waves propagating in inhomogeneous plates with continuously varying thickness. A precise theory was developed to analyze the influence of hysteretic nonlinearity of micro-inhomogeneous material on flexural wave. The difference of the black hole type wedges from the other power law type wedges in the nonlinearity was predicted theoretically. Yuan *et al.* [19] gave a physical model to study the laser-induced surface acoustic wave propagating in roughness surface. The time domain characteristic and the velocity dispersion curve were obtained by using finite element method. The effects of different surface roughnesses on wave velocity were analyzed experimentally. For the problem of Love wave in magneto-electro-elastic layered structures, many researches focused on these structures, such as piezoelectric layer/piezomagnetic half-space or the reverse configuration [20, 21], cylindrically layered struc-

Received 1 June 2016,
accepted 28 July 2016.

© S. Hirzel Verlag · EAA

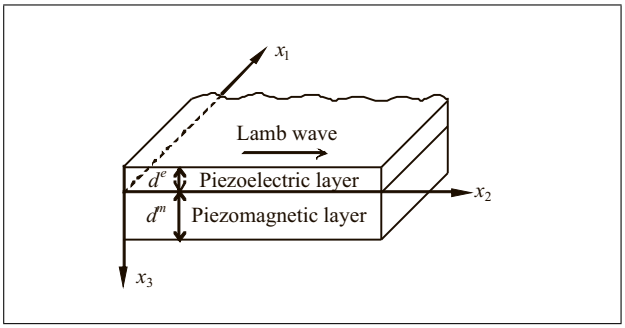


Figure 1. Geometry of a piezoelectric/piezomagnetic bi-material plate.

ture [22], and multilayered structure [23]. Furthermore, effects of initial stress in such layered structures were discussed in [21, 22]. Considering an imperfect bonding, Nie *et al.* [24] studied SH wave propagating in a piezoelectric/piezomagnetic bilayer structure, and the effects of interfacial parameter and electro-magnetic boundary condition on the dispersion behaviors were also discussed. For plane-strain waves, Wu *et al.* [25] and Chen *et al.* [26] investigated Lamb wave propagation in magneto-electro-elastic plate and magneto-electro-elastic multilayered plate, respectively. Cao *et al.* [27] studied Lamb wave in functionally graded piezoelectric-piezomagnetic plate by using the power series technique, and dispersion relations for different boundary conditions are derived in closed form. Zhu *et al.* [28] analyzed the band structure and mode conversion of one-dimensional phononic crystal plates. The behaviors of unidirectional transmission were obtained theoretically in certain frequency bands for both anti-symmetric wave and symmetric wave by employing mode conversion and selection in the linear plate system. Wang *et al.* [29] presented a model to simulate the thermo-elastically generated stress and ultrasound fields in non-metallic materials by using finite element method. The effects of thermal diffusion, optical penetration, and duration of the laser source were analyzed. Pang *et al.* [30] explored Rayleigh-type waves in a piezoelectric layer perfectly bonded on a piezomagnetic half-space. Zhang *et al.* [31] analyzed the effect of initial stress on Rayleigh wave propagating in a magneto-electro-elastic half-space. They found that the initial stresses have strong effect on the phase velocity and magneto-electro-mechanical coupling factor of Rayleigh wave.

However, the interface of layered composites and structures can not be perfectly bonded, due to various causes such as microinhomogeneities, microdefects, and microdebonding, etc. The interfacial imperfection can weaken the interfacial stiffness and continuity, and further affects the wave propagation behavior. Many researches on wave propagation in isotropic elastic media [32] and layered piezoelectric structures [33, 34] with imperfect interfaces have been reported previously. In recent years, Huang *et al.* [35] and Melkumyan *et al.* [36] studied the interfacial shear horizontal wave propagating in a two-phase piezoelectric/piezomagnetic structure. In their works an imperfect interface characterized by the shear-lag model was considered.

The objective of this work is related to the study of the behavior of plane waves in a piezoelectric/piezomagnetic bi-layered plate. Imperfect bonding of the interface is considered. The interface is modeled by the shear-lag model. Exact dispersion relations are obtained using the interface and boundary conditions. The influences of electromagnetic boundary conditions, interfacial parameters and the thickness ratio on dispersion relations are discussed through numerical examples.

2. Problem formulation

2.1. Governing equations

A plate consisting of a piezoelectric layer and a piezomagnetic layer is shown in Figure 1. The constituent materials of the plate are transversely isotropic and are imperfectly bonded along the interface $x_3 = 0$. The thicknesses of piezoelectric layer and piezomagnetic layer are d^e and d^m, respectively. Consider elastic wave propagating in the x_2–x_3 plane. All fields are independent of the x_1-coordinates. The constitutive relations of piezoelectric and piezomagnetic materials can be expressed as follows [26]. For piezoelectric material,

$$\begin{aligned}
\sigma^e_{22} &= c^e_{11}u^e_{2,2} + c^e_{13}u^e_{3,3} + e_{31}\varphi^e_{,3},\\
\sigma^e_{33} &= c^e_{13}u^e_{2,2} + c^e_{33}u^e_{3,3} + e_{33}\varphi^e_{,3},\\
\sigma^e_{23} &= c^e_{44}u^e_{2,3} + c^e_{44}u^e_{3,2} + e_{15}\varphi^e_{,2},\\
D^e_2 &= e_{15}u^e_{2,3} + e_{15}u^e_{3,2} - \in^e_{11}\varphi^e_{,2},\\
D^e_3 &= e_{31}u^e_{2,2} + e_{33}u^e_{3,3} - \in^e_{33}\varphi^e_{,3},\\
B^e_2 &= -\mu^e_{11}\psi^e_{,2},\\
B^e_3 &= -\mu^e_{33}\psi^e_{,3},
\end{aligned} \tag{1}$$

and for piezomagnetic material,

$$\begin{aligned}
\sigma^m_{22} &= c^m_{11}u^m_{2,2} + c^m_{13}u^m_{3,3} + h_{31}\psi^m_{,3},\\
\sigma^m_{33} &= c^m_{13}u^m_{2,2} + c^m_{33}u^m_{3,3} + h_{33}\psi^m_{,3},\\
\sigma^m_{23} &= c^m_{44}u^m_{2,3} + c^m_{44}u^m_{3,2} + h_{15}\psi^m_{,2},\\
D^m_2 &= -\in^m_{11}\varphi^m_{,2},\\
D^m_3 &= -\in^m_{33}\varphi^m_{,3},\\
B^m_2 &= h_{15}u^m_{2,3} + h_{15}u^m_{3,2} - \mu^m_{11}\psi^m_{,2},\\
B^m_3 &= h_{31}u^m_{2,2} + h_{33}u^m_{3,3} - \mu^m_{33}\psi^m_{,3},
\end{aligned} \tag{2}$$

in Equations (1) and (2), u and σ are mechanical displacement and stress, D and φ are electric displacement and electric potential, B and ψ are magnetic flux density and magnetic potential, c, e and h are elastic, piezoelectric and piezomagnetic constants, $\in$ and μ are dielectric permittivity and magnetic permeability, respectively. The superscripts "e" and "m" denote quantities of piezoelectric and piezomagnetic materials. A comma in the subscript indicates the differentiation to the corresponding coordinates.

In the usual quasi-static electro-magnetic approximation, the stress, the electric displacement and the magnetic

flux density satisfy the equation of motion and the Gaussian equations, that is,

$$\begin{aligned} \sigma^{\beta}_{ij,j} &= \rho^{\beta}\frac{\partial^2 u^{\beta}_i}{\partial t^2}, \\ D^{\beta}_{i,i} &= 0, \\ B^{\beta}_{i,i} &= 0, \end{aligned} \tag{3}$$

where t is the time, ρ is the mass density, and $\beta = e, m$.

By substituting Equations (1) and (2) into Equation (3), the governing equations of piezoelectric and piezomagnetic materials can be obtained as

$$\begin{aligned} &c^e_{11}u^e_{2,22} + c^e_{44}u^e_{2,33} \\ &+\left(c^e_{13}+c^e_{44}\right)u^e_{3,23} + \left(e_{15}+e_{31}\right)\varphi^e_{,23} = \rho^e\frac{\partial^2 u^e_2}{\partial t^2}, \\ &\left(c^e_{13}+c^e_{44}\right)u^e_{2,23} + c^e_{44}u^e_{3,22} \\ &+c^e_{33}u^e_{3,33} + e_{15}\varphi^e_{,22} + e_{33}\varphi^e_{,33} = \rho^e\frac{\partial^2 u^e_3}{\partial t^2}, \\ &\left(e_{15}+e_{31}\right)u^e_{2,23} + e_{15}u^e_{3,22} \\ &+e_{33}u^e_{3,33} - \in^e_{11}\varphi^e_{,22} - \in^e_{33}\varphi^e_{,33} = 0, \\ &\mu^e_{11}\psi^e_{,22} + \mu^e_{33}\psi^e_{,33} = 0, \\ &c^m_{11}u^m_{2,22} + c^m_{44}u^m_{2,33} \\ &+\left(c^m_{13}+c^m_{44}\right)u^m_{3,23} + \left(h_{15}+h_{31}\right)\psi^m_{,23} = \rho^m\frac{\partial^2 u^m_2}{\partial t^2}, \\ &\left(c^m_{13}+c^m_{44}\right)u^m_{2,23} + c^m_{44}u^m_{3,22} \\ &+c^m_{33}u^m_{3,33} + h_{15}\psi^m_{,22} + h_{33}\psi^m_{,33} = \rho^m\frac{\partial^2 u^m_3}{\partial t^2}, \\ &\in^m_{11}\varphi^m_{,22} + \in^m_{33}\varphi^m_{,33} = 0, \\ &\left(h_{15}+h_{31}\right)u^m_{2,23} + h_{15}u^m_{3,22} \\ &+h_{33}u^m_{3,33} - \mu^m_{11}\psi^m_{,22} - \mu^m_{33}\varphi^m_{,33} = 0. \end{aligned} \tag{4}$$

$$\tag{5}$$

2.2. Boundary conditions

The shear-lag interface model is introduced to describe the imperfect bonding at the interface. With this model, the stresses at the interface $x_3 = 0$ are continuous but the displacements are discontinuous. In other words, the interface is allowed to deform. So the elastic fields of the interface can be expressed as [33]

$$\begin{aligned} \sigma^e_{23}(x_2,0) &= \sigma^m_{23}(x_2,0) = K_T\left[u^e_2(x_2,0) - u^m_2(x_2,0)\right], \\ \sigma^e_{33}(x_2,0) &= \sigma^m_{33}(x_2,0) = K_N\left[u^e_3(x_2,0) - u^m_3(x_2,0)\right], \end{aligned} \tag{6}$$

where K_T and K_N are the tangential and normal effective elastic stiffnesses of the interface, respectively. K_T and K_N describe how well the two layers are bonded. The infinite values of K_T and K_N represent a prefect interface with continuous displacement across the interface. The degradation of the interfacial properties can be modeled by a reduction in either or both the normal and the tangential elastic stiffnesses. For example, finite values of K_T and K_N represent a imperfect interface, and when they are equal to zero, the interface is without mechanic interaction (zero traction), an unbonded interface is produced. Physically, if the interface is assumed as a separate phase with a extremely small thickness $2h$, then for the shear deformation with respect to the center plane of the thin interface layer, the shear stress-strain relation can be simplified as $\sigma_{23} = G[u_2(x_2,h) - u_2(x_2,-h)]/2h$, where σ_{23} is shear stress and G is the shear modulus of the interface layer. Therefore, the relation between the real interface shear modulus G and the tangential effective elastic stiffness K_T can be expressed as $K_T = G/2h$. Hence, K_T actually represents a combination of the interface elasticity and the thickness [33]. The normal effective elastic stiffness of the interface K_N is also like this.

In addition, the continuity conditions of the electric and magnetic fields at the interface are

$$\begin{aligned} \varphi^e(x_2,0) &= \varphi^m(x_2,0), \\ \psi^e(x_2,0) &= \psi^m(x_2,0), \\ D^e_3(x_2,0) &= D^m_3(x_2,0), \\ B^e_3(x_2,0) &= B^m_3(x_2,0). \end{aligned} \tag{7}$$

The top and bottom surfaces of the plate are assumed to be traction free, which implies that

$$\begin{aligned} \sigma^e_{33}(x_2,-d^e) &= \sigma^e_{23}(x_2,-d^e) = 0, \\ \sigma^m_{33}(x_2,d^m) &= \sigma^m_{23}(x_2,d^m) = 0. \end{aligned} \tag{8}$$

Following the discussions in [13], four kinds of electromagnetic boundary conditions which exist in practical application are considered.

a. Electrically shorted and magnetically open (denoted by "so")

$$\begin{aligned} \varphi^e(x_2,-d^e) &= \psi^e(x_2,-d^e) = 0, \\ \varphi^m(x_2,d^m) &= \psi^m(x_2,d^m) = 0. \end{aligned} \tag{9}$$

b. Electrically and magnetically shorted (denoted by "ss")

$$\begin{aligned} \varphi^e(x_2,-d^e) &= B^e_3(x_2,-d^e) = 0, \\ \varphi^m(x_2,d^m) &= B^m_3(x_2,d^m) = 0. \end{aligned} \tag{10}$$

c. Electrically and magnetically open (denoted by "oo")

$$\begin{aligned} D^e_3(x_2,-d^e) &= \psi^e(x_2,-d^e) = 0, \\ D^m_3(x_2,d^m) &= \psi^m(x_2,d^m) = 0. \end{aligned} \tag{11}$$

d. Electrically open and magnetically shorted (denoted by "os")

$$\begin{aligned} D^e_3(x_2,-d^e) &= B^e_3(x_2,-d^e) = 0, \\ D^m_3(x_2,d^m) &= B^m_3(x_2,d^m) = 0. \end{aligned} \tag{12}$$

3. Fields in piezoelectric/piezomagnetic layers and dispersion relation

3.1. Fields in piezoelectric layer

Consider plane waves propagating in the x_2-direction. By the partial wave method [37], solutions to the piezoelectric

governing equations (4) can be expressed as

$$\begin{aligned} u_2^e(x_2,x_3,t) &= A_1^e\, e^{b^e k x_3}\cos\big[k(x_2-ct)\big],\\ u_3^e(x_2,x_3,t) &= A_2^e\, e^{b^e k x_3}\sin\big[k(x_2-ct)\big],\\ \varphi^e(x_2,x_3,t) &= A_3^e\, e^{b^e k x_3}\sin\big[k(x_2-ct)\big],\\ \psi^e(x_2,x_3,t) &= A_4^e\, e^{b^e k x_3}\sin\big[k(x_2-ct)\big], \end{aligned} \tag{13}$$

where k is the wave number. c is the phase velocity. A_i^e ($i = 1...4$) are unknown amplitudes. b^e is a parameter to be determined. Substitution of Equation (13) into Equation (4) gives

$$\begin{aligned} \big(c_{44}^e b^{e2} - c_{11}^e + \rho^e c^2\big)A_1^e + \big(c_{13}^e + c_{44}^e\big)b^e A_2^e \\ +\big(e_{15}+e_{31}\big)b^e A_3^e &= 0,\\ \big(c_{13}^e + c_{44}^e\big)b^e A_1^e + \big(c_{44}^e - c_{33}^e b^{e2} - \rho^e c^2\big)A_2^e \\ +\big(e_{15}-e_{33}b^{e2}\big)A_3^e &= 0,\\ \big(e_{15}+e_{33}\big)b^e A_1^e + \big(e_{15}-e_{33}b^{e2}\big)A_2^e \\ +\big(\ \epsilon_{33}^e\ b^{e2} - \epsilon_{11}^e\ \big)A_3^e &= 0,\\ \big(\mu_{33}^e b^{e2} - \mu_{11}^e\big)A_4^e &= 0. \end{aligned} \tag{14}$$

From the above equations, it is found that the last equation is uncoupled with the other three. For $A_4^e \neq 0$, the parameter b^e can be solved from the last equation in (14) as a pair of real roots with opposite signs, i.e. $b^e = \pm\sqrt{\mu_{11}^e/\mu_{33}^e}$. The positive and negative signs correspond to increasing and decaying magnetic potentials, respectively.

A nontrivial solution for A_i^e ($i = 1\ldots3$) requires that the determinant of the coefficients matrix must vanish, i.e.

$$\begin{vmatrix} c_{44}^e b^{e2} - c_{11}^e + \rho^e c^2 & (c_{13}^e + c_{44}^e)b^e & (e_{15}+e_{31})b^e \\ (c_{13}^e + c_{44}^e)b^e & c_{44}^e - c_{33}^e b^{e2} - \rho^e c^2 & e_{15} - e_{33}b^{e2} \\ (e_{15}+e_{31})b^e & e_{15} - e_{33}b^{e2} & \epsilon_{33}^e\, b^{e2} - \epsilon_{11}^e \end{vmatrix} = 0. \tag{15}$$

Equation (15) is a six-order equation in b^e with phase velocity c as the unknown parameter. Thus, for a given value of c, there are six roots that satisfy Equation (15). They are denoted by b_j^e ($j = 1\ldots6$). Substituting the roots of b^e into the first two of Equation (14), the amplitude ratios A_{1j}^e/A_{3j}^e and A_{2j}^e/A_{3j}^e can be obtained as

$$A_{1j}^e = S_{1j}^e A_{3j}^e, \quad A_{2j}^e = S_{2j}^e A_{3j}^e, \tag{16}$$

where $S_{1j}^e = s_{1j}^e/s_j^e$, $S_{2j}^e = s_{2j}^e/s_j^e$. The expressions of s_j^e, s_{1j}^e and s_{2j}^e are listed in Appendix A1.

The complete solutions for the piezoelectric layer must involve all the eight roots of b^e. Let $b_7^e = -b_8^e = \sqrt{\mu_{11}^e/\mu_{33}^e}$. The displacement, electric and magnetic potentials are given by

$$\begin{aligned} u_2^e(x_2,x_3,t) &= \sum_{j=1}^{6} A_{3j}^e S_{1j}^e\, e^{b_j^e k x_3}\cos\big[k(x_2-ct)\big],\\ u_3^e(x_2,x_3,t) &= \sum_{j=1}^{6} A_{3j}^e S_{2j}^e\, e^{b_j^e k x_3}\sin\big[k(x_2-ct)\big], \end{aligned}$$

$$\begin{aligned} \varphi^e(x_2,x_3,t) &= \sum_{j=1}^{6} A_{3j}^e\, e^{b_j^e k x_3}\sin\big[k(x_2-ct)\big], \\ \psi^e(x_2,x_3,t) &= \sum_{n=7}^{8} A_{4n}^e\, e^{b_n^e k x_3}\sin\big[k(x_2-ct)\big]. \end{aligned} \tag{17}$$

By substituting Equation (17) into Equation (1), the stress, electric displacement and magnetic flux density can be obtained as

$$\begin{aligned} \sigma_{33}^e &= \sum_{j=1}^{6}\big(-c_{13}^e S_{1j}^e + c_{33}^e b_j^e S_{2j}^e + e_{33}b_j^e\big) \\ &\quad\cdot k\, e^{b_j^e k x_3} A_{3j}^e \sin\big[k(x_2-ct)\big],\\ \sigma_{23}^e &= \sum_{j=1}^{6}\big[c_{44}^e\big(b_j^e S_{1j}^e + S_{2j}^e\big) + e_{15}\big] \\ &\quad\cdot k\, e^{b_j^e k x_3} A_{3j}^e \cos\big[k(x_2-ct)\big],\\ D_3^e &= \sum_{j=1}^{6}\big(-e_{31}S_{1j}^e + e_{33}b_j^e S_{2j}^e - \epsilon_{33}^e\, b_j^e\big) \\ &\quad\cdot k\, e^{b_j^e k x_3} A_{3j}^e \sin\big[k(x_2-ct)\big], \\ B_3^e &= -\sum_{n=7}^{8}\mu_{33}^e b_n^e k\, e^{b_n^e k x_3} A_{4n}^e \sin\big[k(x_2-ct)\big]. \end{aligned} \tag{18}$$

3.2. Fields in piezomagnetic layer

In a similar way, solutions for the piezomagnetic layer are obtained as

$$\begin{aligned} u_2^m(x_2,x_3,t) &= \sum_{j=1}^{6} A_{4j}^m S_{1j}^m\, e^{b_j^m k x_3}\cos\big[k(x_2-ct)\big],\\ u_3^m(x_2,x_3,t) &= \sum_{j=1}^{6} A_{4j}^m S_{2j}^m\, e^{b_j^m k x_3}\sin\big[k(x_2-ct)\big],\\ \varphi^m(x_2,x_3,t) &= \sum_{n=7}^{8} A_{3n}^m\, e^{b_n^m k x_3}\sin\big[k(x_2-ct)\big], \\ \psi^m(x_2,x_3,t) &= \sum_{j=1}^{6} A_{4j}^m\, e^{b_j^m k x_3}\sin\big[k(x_2-ct)\big]. \end{aligned} \tag{19}$$

Substituting Equation (19) into Equation (2), the stress, electric displacement and magnetic flux density for piezomagnetic layer can be obtained as

$$\begin{aligned} \sigma_{33}^m &= \sum_{j=1}^{6}\big(-c_{13}^m S_{1j}^m + c_{33}^m b_j^m S_{2j}^m + h_{33}b_j^m\big) \\ &\quad\cdot k\, e^{b_j^m k x_3} A_{4j}^m \sin\big[k(x_2-ct)\big],\\ \sigma_{23}^m &= \sum_{j=1}^{6}\big[c_{44}^m\big(b_j^m S_{1j}^m + S_{2j}^m\big) + h_{15}\big] \\ &\quad\cdot k\, e^{b_j^m k x_3} A_{4j}^m \cos\big[k(x_2-ct)\big],\\ D_3^m &= -\sum_{n=7}^{8}\epsilon_{33}^m\, b_n^m k\, e^{b_n^m k x_3} A_{3n}^m \sin\big[k(x_2-ct)\big], \end{aligned}$$

$$B_3^m = \sum_{j=1}^{6} \left(-h_{31} S_{1j}^m + h_{33} b_j^m S_{2j}^m - \mu_{33}^m b_j^m \right) \cdot k\, e^{b_j^m k x_3} A_{4j}^m \sin\left[k(x_2 - ct)\right], \quad (20)$$

where $b_7^m = -b_8^m = \sqrt{\epsilon_{11}^m / \epsilon_{33}^m}$, $S_{1j}^m = s_{1j}^m / s_j^m$, and $S_{2j}^m = s_{2j}^m / s_j^m$. The expressions of s_j^m, s_{1j}^m and s_{2j}^e are given in Appendix A2.

3.3. Dispersion relation

Substituting these solutions of piezoelectric and piezomagnetic materials obtained in the previous section into the interface conditions (6)–(7) as well as the boundary conditions (8)–(12). For any one of the four kinds of different electro-magnetic boundary conditions, a system of sixteen linear homogeneous algebraic equations with undetermined constants A_{3j}^e, A_{4j}^m ($j = 1 \ldots 6$) and A_{4n}^e, A_{3n}^m ($n = 7, 8$) can be obtained, i.e.,

$$\boldsymbol{M}\, \boldsymbol{A} = 0, \quad (21)$$

where

$$\boldsymbol{A} = \left[A_{44}^m, A_{31}^e, A_{32}^e, A_{33}^e, A_{34}^e, A_{35}^e, A_{36}^e, A_{47}^e, A_{48}^e, A_{41}^m, A_{42}^m, A_{43}^m, A_{45}^m, A_{46}^m, A_{37}^m, A_{38}^m\right]^{\mathrm{T}}$$

is a vector consisting of undetermined constants, $\boldsymbol{M}$ is a 16×16 matrix. For brevity, only the elements of $\boldsymbol{M}$ for the "so" electro-magnetic boundary condition are listed in Appendix A3. A nontrivial solution for $\boldsymbol{A}$ requires that the determinant of the coefficients matrix must vanish, i.e.,

$$\left| \boldsymbol{M} \right| = 0. \quad (22)$$

The above equation gives a relation for phase velocity versus wave number, which is the dispersion equation. However, because of the complexity, the dispersion equation can only be numerically solved. According to the solving procedure in [37], we firstly assign a fixed value to the non-dimensional wave number kd^m, e.g. $kd^m = k_0$, and then give a smaller estimated value of phase velocity c, for example, $c = c_0$. By substituting the two given values into the left hand of Equation (22), a positive or a negative solution m_0 can be obtained. Subsequently, impart another slightly larger value to c, e.g. $c_1 > c_0$, recalculate the left hand of Equation (22), another solution m_1 can be obtained. If m_0 and m_1 are synchronously positive or negative, continue to enlarge the value of c_1 until m_0 and m_1 turn into opposite sign. Finally, the dichotomy is employed to approach the exact phase velocity c in the certain interval $c_0 < c < c_1$. This root of c is the solution of the lowest mode corresponding to the given non-dimensional wave number k_0. For the higher modes, by assigning a larger value of c_2 to c, e.g. $c_2 > c_1$, we can continue to seek the solutions of phase velocity one by one in the certain interval $c_1 < c < c_2$. By circulating the above processes, the solutions of phase velocity corresponding to different values of non-dimensional wave number can be obtained.

Table I. Material properties used in numerical examples.

Parameters	$BaTiO_3$	$CoFe_2O_4$
c_{11} (10^9 N/m^2)	166	286
c_{13} (10^9 N/m^2)	78	170
c_{33} (10^9 N/m^2)	162	269.5
c_{44} (10^9 N/m^2)	43	45.3
e_{15} (C/m^2)	11.6	–
e_{31} (C/m^2)	-4.4	–
e_{33} (C/m^2)	18.6	–
h_{15} (N/A m)	–	550
h_{31} (N/A m)	–	580.3
h_{33} (N/A m)	–	699.7
ϵ_{11} (10^{-9} C^2/N m^2)	11.2	0.08
ϵ_{33} (10^{-9} C^2/N m^2)	12.6	0.093
μ_{11} (10^{-6} N s^2/C^2)	5	157
μ_{33} (10^{-6} N s^2/C^2)	10	157
ρ (10^3 kg/m^3)	5.8	5.3
c_{sh} (m/s)	3079.81	2985.08
c_R (m/s)	2758.21 ($\varphi = 0$)	2837.76 ($\psi = 0$)
	2792.33 ($D = 0$)	2845.05 ($B = 0$)

4. Numerical examples and discussions

In this section, the effects of the electro-magnetic boundary conditions, the interface characteristics and the thickness ratio on dispersion relations are examined in detail using the obtained dispersion relations. The piezoelectric and piezomagnetic materials used in numerical examples are $BaTiO_3$ and $CoFe_2O_4$, respectively. The material properties are listed in Table I [26, 38]. For convenience, the corresponding bulk shear wave velocitiy c_{sh} and the Rayleigh surface wave velocity c_R of $BaTiO_3$ and $CoFe_2O_4$ are also presented in Table I. Two non-dimensional parameters are introduced to describing the tangential and normal interface bonding and are defined as $\alpha = K_T d^m / c_{44}^m$ and $\beta = K_N d^m / c_{44}^m$, respectively. In the following figures, the horizontal axis is the non-dimensional wave number kd^m. The vertical axis is the phase velocity c. f is the thickness ratio of the piezoelectric layer to the piezomagnetic layer.

4.1. Effect of electro-magnetic boundary condition

The dispersion curves of the first three modes for four kinds of electro-magnetic boundary conditions are shown in Figure 2, where the interface between piezoelectric layer and piezomagnetic layer is perfect bonding, and the thickness ratio f is equal to 1. From Figure 2a, it can be seen that dispersion curves of the first mode for the same electric boundary conditions are almost consistent, that is to say, "so" case is close to "ss" case, and "oo" case is close to "os" case. The phase velocity increases with the non-dimensional wave number increasing. The phase velocities for "so" and "ss" cases tend to the Rayleigh surface wave velocity of $BaTiO_3$ for electrically shorted boundary condition (2758.21 m/s) at the larger wave number. While, the phase velocities for "oo" and "os" cases approach the Rayleigh surface wave velocity of $BaTiO_3$ for electrically open boundary condition (2792.33 m/s). Furthermore, the phase velocity of the electrically open case is larger than

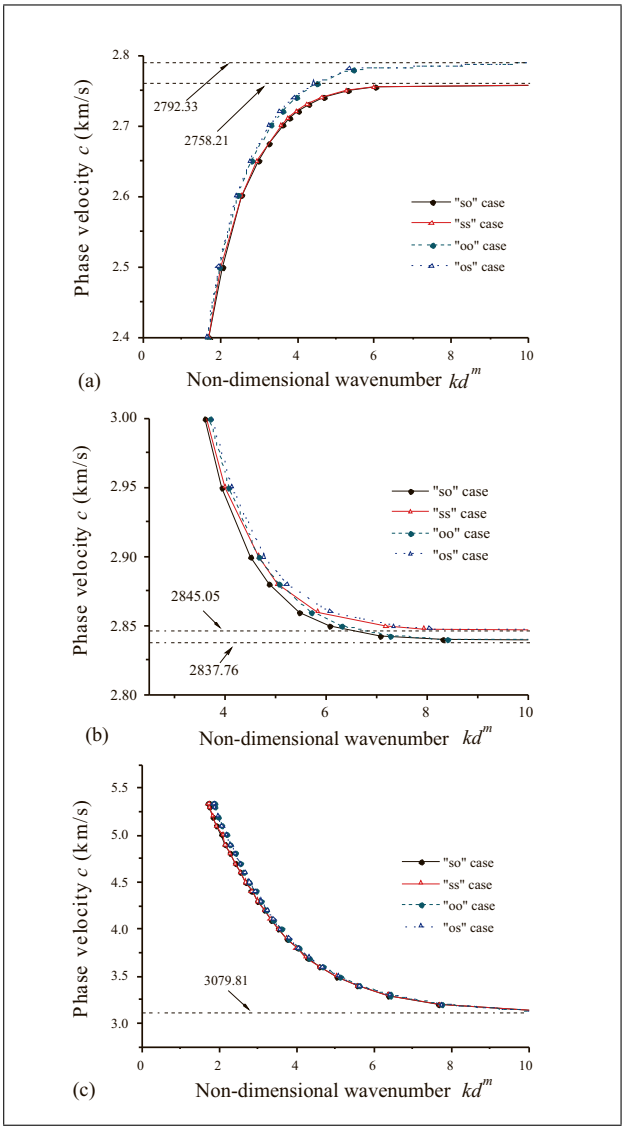


Figure 2. Dispersion curves of the first three modes for kinds of electro-magnetic boundary conditions with perfect interface, where $f = 1$. (a) First mode, (b) second mode, (c) third mode.

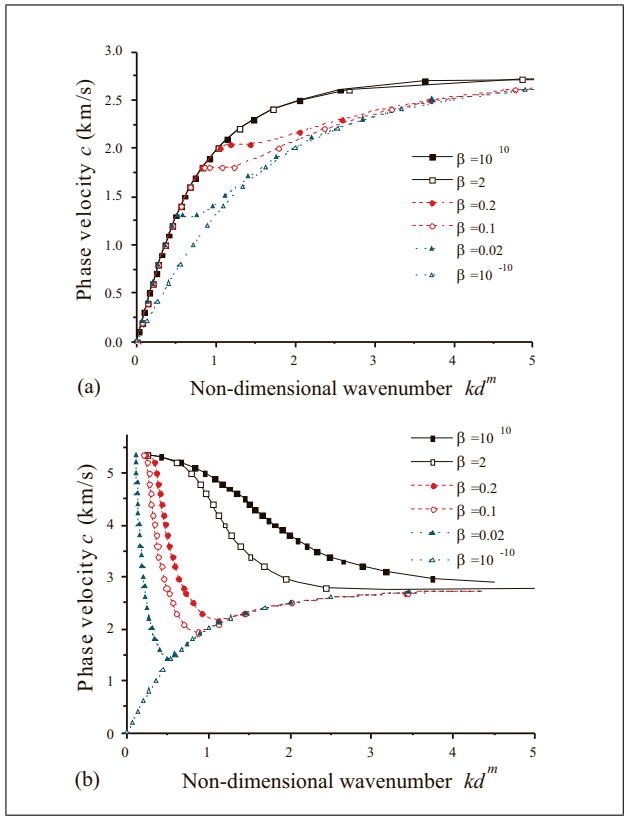


Figure 3. Dispersion curves of the first two modes for normal imperfect bonding, where $f = 1$. (a) First mode, (b) second mode.

that of the electrically shorted case. From Figure 2b, it is found that the dispersion curves of the second mode for the same magnetic boundary conditions are nearly consistent in the range of larger non-dimensional wave numbers, that is, "so" case approximates to "oo" case, and "ss" case approximates to "os" case. Different from the first mode, the phase velocity of the second mode decreases with the non-dimensional wave number increasing. The phase velocities for "so" and "oo" cases fall towards the Rayleigh surface wave velocity of $CoFe_2O_4$ for magnetically open boundary condition (2837.76 m/s) at the larger wave number. While, the phase velocities for "ss" and "os" cases approach the Rayleigh surface wave velocity of $CoFe_2O_4$ for magnetically shorted boundary condition (2845.05 m/s). Moreover, the phase velocities of the magnetically shorted case are slightly larger than that of the magnetically open case. For the third mode, it can be seen from Figure 2c that the dispersion curves for the considered four kinds of electro-magnetic boundary conditions are nearly consistent, and uniformly approach the bulk shear wave velocity of $BaTiO_3$ regardless of the electro-magnetic boundary conditions.

Based on the above analysis, it is found that the electro-magnetic boundary conditions play a dominant role in the dispersion relation of Lamb wave. Therefore, we can deduce that, for Lamb wave propagating in a $BaTiO_3/CoFe_2O_4$ bi-material plate, the first mode and second mode can respectively be determined by the electric and magnetic boundary conditions, and the third mode has nothing to do with the electro-magnetic boundary conditions. In order to deeply reveal the effects of imperfect interface and thickness ratio on the dispersion behavior of Lamb wave, we separately calculate four kinds of dispersion relations for "so", "ss", "oo", and "os" electro-magnetic boundary conditions with different interface parameters and thickness ratios. It is found that the trends of change for different electro-magnetic boundary conditions are close resemblance. However, due to their superposition together, we only plot to illustrate the case of "so" boundary condition in the following discussions and the other situations are not presented here.

4.2. Effect of interface property

Figures 3a and 3b present the effects of the normal interfacial parameter on the dispersion curves of the first two modes, where β is taken as 10^{-10}, 0.02, 0.1, 0.2, 2, and 10^{10}, respectively, and $f = 1$. The figures show that the

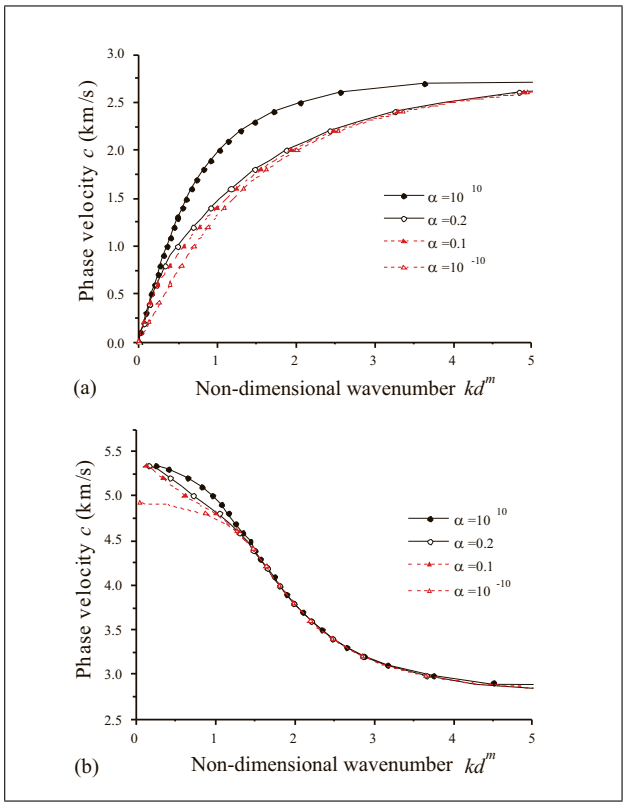


Figure 4. Dispersion curves of the first two modes for tangential imperfect bonding, where $f = 1$. (a) First mode, (b) second mode.

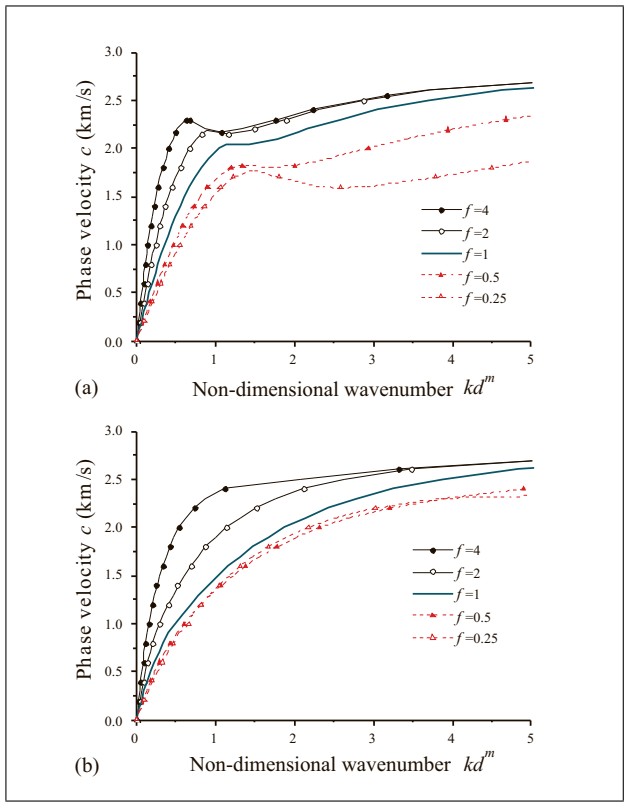


Figure 5. Dispersion curves of the first mode for different thickness ratios. (a) Normal imperfect bonding ($\alpha = 10^{10}$, $\beta = 0.2$). (b) Tangential imperfect bonding ($\alpha = 0.2$, $\beta = 10^{10}$).

imperfect bonding reduces the wave velocities, in particular, the approximate debonding interface as $\beta = 10^{-10}$. Moreover, the weaker the interface bonding, the smaller the phase velocity of Lamb wave propagating. It is due to the fact that the imperfect bonding represents a deformable interface and is less stiff compared with an interface with perfect bonding. In addition, the influence of the normal imperfect bonding on the second mode is larger than that of the first mode.

The effects of the tangential imperfect bonding on dispersion curves of the first two modes are shown in Figure 4a and 4b, respectively, where $\alpha = 10^{-10}$, 0.1, 0.2, 10^{10}, and $f = 1$. Compared with the effects of the normal imperfect bonding shown in Figure 3, it is observed that the tangential interfacial parameter has smaller effects on dispersion curves. This is because the tangential imperfect bonding only results in sliding contact, while the normal imperfect bonding maybe produce the interfacial detachment, and strongly affect the propagation of Lamb wave. This feature is similar to that of Lamb waves in elastic bilayer plate with imperfect interface obtained by Deng [32]. In particular it has no effect on the second mode when the wave number is relatively larger.

4.3. Effect of the thickness ratio

Effects of the thickness ratio on dispersion curves of the first mode with normal and tangential imperfections are shown in Figures 5a and 5b, respectively, where the thickness ratio is taken as 0.25, 0.5, 1, 2 and 4, respectively. It is found that the larger the thickness ratio, the larger the phase velocity of the first mode is. Effects of the thickness ratio on the second mode are shown in Figure 6. For tangential imperfect bonding, it is clear that the smaller the thickness ratio, the larger the phase velocity is. In case of normal imperfect bonding, the influences and changes become complexity. When the wave number is small, the behavior is similar to those of tangential imperfect bonding. There is a lowest velocity of second mode for every different thickness ratios. However, these minimum values are corresponding to different non-dimensional wave numbers. At the larger wave number, the velocities of the second mode approach the Rayleigh surface wave velocity of $CoFe_2O_4$ for magnetically open boundary condition regardless of the thickness ratio.

5. Conclusions

Propagation of Lamb wave in a piezoelectric/piezomagnetic bi-material plate with an imperfect interface is studied. Exact dispersion ration is established in matrix form. The effects of electro-magnetic boundary condition, interfacial parameter, and thickness ratio on dispersion relation are examined and discussed numerically. The results show that the first two modes are separately determined by the electric and magnetic boundary conditions, and the third mode has nothing to do with the electro-magnetic boundary conditions. The imperfection existed in bonding interface can greatly reduce the velocity of Lamb wave in cer-

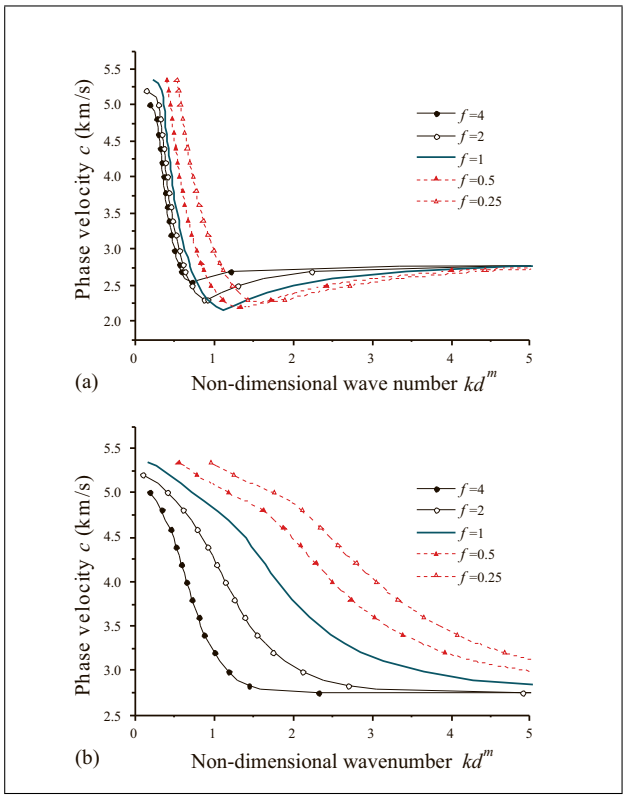


Figure 6. Dispersion curves of the second mode for different thickness ratios. (a) Normal imperfect bonding ($\alpha = 10^{10}$, $\beta = 0.2$). (b) Tangential imperfect bonding ($\alpha = 0.2$, $\beta = 10^{10}$).

tain range of wave number. The weaker the interface bonding, the smaller the phase velocity of Lamb wave propagating in the corresponding bilayer structure. The dispersion relations are more sensitive to the normal interfacial parameter comparing to the tangential parameter. The thickness ratio of the piezoelectric layer to the piezomagnetic layer has great effect on the dispersion relation. For the first mode of Lamb wave, the larger the thickness ratio, the larger the phase velocity is.

Acknowledgements

This work is supported by the National Nature Science Foundation of China (11272221, 10972147), and the Natural Science Foundation of Hebei Province of China (A2013210106).

Appendix

A1. Expressions of s_j^e, s_{1j}^e and s_{2j}^e

$$s_j^e = \begin{vmatrix} c_{44}^e b_j^{e2} - c_{11}^e + \rho^e c^2 & (c_{13}^e + c_{44}^e) b_j^e \\ (c_{13}^e + c_{44}^e) b_j^e & c_{44}^e - c_{33}^e b_j^{e2} - \rho^e c^2 \end{vmatrix},$$

$$s_{1j}^e = \begin{vmatrix} -(e_{15} + e_{31}) b_j^e & (c_{13}^e + c_{44}^e) b_j^e \\ -(e_{15} - e_{33} b_j^{e2}) & c_{44}^e - c_{33}^e b_j^{e2} - \rho^e c^2 \end{vmatrix},$$

$$s_{2j}^e = \begin{vmatrix} c_{44}^e b_j^{e2} - c_{11}^e + \rho^e c^2 & -(e_{15} + e_{31}) b_j^e \\ (c_{13}^e + c_{44}^e) b_j^e & -(e_{15} - e_{33} b_j^{e2}) \end{vmatrix}.$$

A2. Expressions of s_j^m, s_{1j}^m and s_{2j}^m

$$s_j^m = \begin{vmatrix} c_{44}^m b_j^{m2} - c_{11}^m + \rho^m c^2 & (c_{13}^m + c_{44}^m) b_j^m \\ (c_{13}^m + c_{44}^m) b_j^m & c_{44}^m - c_{33}^m b_j^{m2} - \rho^m c^2 \end{vmatrix},$$

$$s_{1j}^m = \begin{vmatrix} -(h_{15} + h_{31}) b_j^m & (c_{13}^m + c_{44}^m) b_j^m \\ -h_{15} - h_{33} b_j^{m2} & c_{44}^m - c_{33}^m b_j^{m2} - \rho^m c^2 \end{vmatrix},$$

$$s_{2j}^m = \begin{vmatrix} c_{44}^m b_j^{m2} - c_{11}^m + \rho^m c^2 & -(h_{15} + h_{31}) b_j^m \\ (c_{13}^m + c_{44}^m) b_j^m & -h_{15} - h_{33} b_j^{m2} \end{vmatrix}.$$

A3. Elements of matrix $\boldsymbol{M}$ for the "so" electromagnetic boundary condition, denoted by $m_{k,l}$ $(k, l = 1 \ldots 16)$

Let:
$$\begin{aligned} P_l^e &= -c_{13}^e S_{1l}^e + c_{33}^e b_l^e S_{2l}^e + e_{33} b_l^e, \\ R_l^e &= c_{44}^e \left(b_l^e S_{1l}^e + S_{2l}^e \right) + e_{15}, \\ T_l^e &= -e_{31} S_{1l}^e + e_{33} b_l^e S_{2l}^e - \epsilon_{33}^e b_l^e, \\ P_l^m &= -c_{13}^m S_{1l}^m + c_{33}^m b_l^m S_{2l}^m + h_{33} b_l^m, \\ R_l^m &= c_{44}^m \left(b_l^m S_{1l}^m + S_{2l}^m \right) + h_{15}, \\ T_l^m &= -h_{31} S_{1l}^m + h_{33} b_l^m S_{2l}^m - \mu_{33}^m b_l^m, \end{aligned}$$

then

$$m_{1,l} = P_l^e \exp\left(- b_l^e k d^m f \right), \quad m_{2,l} = R_l^e \exp\left(- b_l^e k d^m f \right),$$
$$m_{3,l} = \exp\left(- b_l^e k d^m f \right), \quad m_{9,l} = S_{1l}^e, \quad m_{10,l} = S_{2l}^e,$$
$$m_{11,l} = P_l^e, \quad m_{12,l} = R_l^e, \quad m_{13,l} = 1, \quad m_{15,l} = T_l^e,$$
$$(l = 1 \ldots 6).$$
$$m_{5,l} = P_{l-8}^m \exp\left(b_{l-8}^m k d^m \right),$$
$$m_{6,l} = R_{l-8}^m \exp\left(b_{l-8}^m k d^m \right),$$
$$m_{8,l} = \exp\left(b_{l-8}^m k d^m \right), \quad m_{9,l} = R_{l-8}^e - \left(\alpha / k d^m \right) S_{1,l-8}^m,$$
$$m_{10,l} = P_{l-8}^e - \left(\beta / k d^m \right) S_{2,l-8}^m, \quad m_{11,l} = -P_{l-8}^m,$$
$$m_{12,l} = -R_{l-8}^m, \quad m_{14,l} = -1, \quad m_{16,l} = -T_{l-8}^m,$$
$$(l = 9 \ldots 14).$$
$$m_{4,7} = \exp\left(\sqrt{\mu_{11}^e / \mu_{33}^e} k d^m f \right),$$
$$m_{4,8} = \exp\left(- \sqrt{\mu_{11}^e / \mu_{33}^e} k d^m f \right),$$
$$m_{7,15} = \exp\left(- \sqrt{\epsilon_{11}^m / \epsilon_{33}^m} k d^m \right),$$
$$m_{7,16} = \exp\left(\sqrt{\epsilon_{11}^m / \epsilon_{33}^m} k d^m \right),$$
$$m_{13,15} = m_{13,16} = -1, \quad m_{14,7} = m_{14,8} = 1,$$
$$m_{15,15} = -\sqrt{\epsilon_{11}^m \epsilon_{33}^m}, \quad m_{15,16} = \sqrt{\epsilon_{11}^m \epsilon_{33}^m},$$
$$m_{16,7} = \sqrt{\mu_{11}^e \mu_{33}^e}, \quad m_{16,8} = -\sqrt{\mu_{11}^e \mu_{33}^e}.$$

The other elements of Matrix $\boldsymbol{M}$ are zero.

References

[1] J. V. Suchtelen: Product properties: A new application of composite materials. Philips Research Reports **27** (1972) 28–37.

[2] M. I. Bichurin, V. M. Petrov, R. V. Petrov, et al.: Magnetoelectric microwave devices. Ferroelectrics **280** (2002) 211–218.

[3] Y. K. Fetisov, G. Srinivasan: Electric field tuning characteristics of a ferrite-piezoelectric microwave resonator. Applied Physics Letters **88** (2006) 143503.

[4] A. S. Tatarenko, M. I. Bichurin, G. Srinivasan: Electrically tunable microwave filters based on ferromagnetic resonance in ferrite-ferroelectric bilayers. Electronics Letters **41** (2005) 596–598.

[5] S. X. Dong, J. F. Li, D. Viehland: Circumferentially magnetized and circumferentially polarized magnetostrictive/piezoelectric laminated rings. Journal of Applied Physics **96** (2004) 3382–3387.

[6] S. X. Dong, J. Y. Zhai, F. M. Bai, et al.: Push-pull mode magnetostrictive/piezoelectric laminate composite with an enhanced magnetoelectric voltage coefficient. Applied Physics Letters **87** (2005) 062502.

[7] J. G. Wan, J. M. Liu, G. H. Wang, et al.: Electric-field-induced magnetization in $Pb(Zr,Ti)O_3$/Terfenol-D composite structures. Applied Physics Letters **88** (2006) 182505.

[8] S. X. Dong, J. F. Li, D. Viehland: Voltage gain effect in a ring-type magnetoelectric laminate. Applied Physics Letters **84** (2004) 4188–4190.

[9] S. X. Dong, J. F. Li, D. Viehland: A strong magnetoelectric voltage gain effect in magnetostrictive-piezoelectric composite. Applied Physics Letters **85** (2004) 3534–3536.

[10] W. Eerenstein, N. D. Mathur, J. F. Scott: Multiferroic and magnetoelectric materials. Nature **442** (2006) 759–765.

[11] M. Fiebig: Revival of the magnetoelectric effect. Journal of Physics D: Applied Physics **38** (2005) R123–R152.

[12] C. W. Nan, M. I. Bichurin, S. X. Dong, et al.: Multiferroic magnetoelectric composites: Historical perspective, status, and future directions. Journal of Applied Physics **103** (2008) 031101.

[13] V. I. Alshits, A. N. Darinskii, J. Lothe: On the existence of surface waves in half-infinite anisotropic elastic media with piezoelectric and piezomagnetic properties. Wave Motion **16** (1992) 265–283.

[14] A. Melkumyan: Twelve shear surface waves guided by clamped/free boundaries in magneto-electro-elastic materials. International Journal of Solids and Structures **44** (2007) 3594–3599.

[15] J. X. Liu, D. N. Fang, X. L. Liu: A shear horizontal surface wave in magnetoelectric materials. IEEE Transactions on Ultrasonics, Ferroelectrics, and Frequency Control **54** (2007) 1287–1289.

[16] B. L. Wang, Y. W. Mai, O. P. Niraula: A horizontal shear surface wave in magnetoelectroelastic materials. Philosophical Magazine Letters **87** (2007) 53–58.

[17] A. K. Soh, J. X. Liu: Interfacial shear horizontal waves in a piezoelectric-piezomagnetic bi-material. Philosophical Magazine Letters **86** (2006) 31–35.

[18] V. E. Gusev, C. Y. Ni, A. Lomonosov, et al.: Propagation of flexural waves in inhomogeneous plates exhibiting hysteretic nonlinearity: Nonlinear acoustic black holes. Ultrasonics **61** (2015) 126–135.

[19] L. Yuan, K. H. Sun, Y. P. Cui, et al.: Experimental and theoretical analysis of the dispersion of laser-induced surface acoustic wave due to surface roughness. Acta Physica Sinica **61** (2012) 014210.

[20] J. X. Liu, D. N. Fang, W. Y. Wei, et al.: Love waves in layered piezoelectric/piezomagnetic structures. Journal of Sound and Vibration **315** (2008) 146–156.

[21] J. Du, X. Jin, J. Wang: Love wave propagation in layered magneto-electro-elastic structures with initial stress. Acta Mechanica **192** (2007) 169–189.

[22] J. K. Du, K. Xian, J. Wang: Love wave propagation in a cylindrically layered magneto-electro-elastic structure. Proceedings-IEEE Ultrasonics Symposium, 2007, 1641–1644.

[23] J. Y. Chen, H. L. Chen: Love wave propagation in magneto-electro-elastic multilayered structure (in Chinese). Acta Materiae Compositae Sinica **23** (2006) 181–184.

[24] G. Q. Nie, J. X. Liu, X. Q. Fang, et al.: Shear horizontal (SH) waves propagating in piezoelectric–piezomagnetic bilayer system with an imperfect interface. Acta Mechanica **223** (2012) 1999–2009.

[25] X. H. Wu, Y. P. Shen, Q. Sun: Lamb wave propagation in magnetoelectroelastic plates. Applied Acoustics **68** (2007) 1224–1240.

[26] J. Y. Chen, E. Pan, H. L. Chen: Wave propagation in magneto-electro-elastic multilayered plates. International Journal of Solids and Structures **44** (2007) 1073–1085.

[27] X. S. Cao, J. P. Shi, F. Jin: Lamb wave propagation in the functionally graded piezoelectric–piezomagnetic material plate. Acta Mechanica **223** (2012) 1081–1091.

[28] X. F. Zhu, X. Y. Zou, B. Liang, et al.: One-way mode transmission in one-dimensional phononic crystal plates. Journal of Applied Physics **108** (2010) 124909.

[29] J. Wang, Z. Shen, B. Xu, et al.: Simulation on thermoelastic stress field and laser ultrasound waveform in non-metallic materials by using FEM. Applied Physics A: Materials Science and Processing **84** (2006) 301–307.

[30] Y. Pang, J. X. Liu, Y. S. Wang, et al.: Propagation of Rayleigh-type surface waves in a transversely isotropic piezoelectric layer on a piezomagnetic half-space. Journal of Applied Physics **103** (2008) 074901.

[31] R. Zhang, Y. Pang, W. J. Feng: Propagation of Rayleigh waves in a magneto-electro-elastic half-space with initial stress. Mechanics of Advanced Materials and Structures **21** (2014) 538–543.

[32] M. X. Deng: Analysis of second-harmonic generation of Lamb waves propagating in layered planar structures with imperfect interfaces. Applied Physics Letters **88** (2006) 221902.

[33] Z. G. Chen, Y. T. Hu, J. S. Yang: Shear horizontal piezoelectric waves in a piezoceramic plate imperfectly bonded to two piezoceramic half-spaces. Journal of Mechanics **24** (2008) 229–239.

[34] L. M. Xu, H. Fan, M. Chen, et al.: Modeling piezoelectric interfacial wave near an imperfect interface. Journal of Electronic Science and Technology of China **4** (2006) 269–273.

[35] Y. Huang, X. F. Li, K. Y. Lee: Interfacial shear horizontal (SH) waves propagating in a two-phase piezoelectric/piezomagnetic structure with an imperfect interface. Philosophical Magazine Letters **89** (2009) 95–103.

[36] A. Melkumyan, Y. W. Mai: Influence of imperfect bonding on interface waves guided by piezoelectric/piezomagnetic composites. Philosophical Magazine **88** (2008) 2965–2977.

[37] J. L. Rose: Ultrasonic wave in solid media. Cambridge University Press, 1999.

[38] G. D. Luan, J. D. Zhang, R. Q. Wang: Transducer piezoelectric and arrays (revised edition) (in Chinese). Peking University Press, 2005.